Epitaxial Graphene Growth on the Step-Structured Surface of Off-Axis C-Face 3C-SiC($\bar{1}\,\bar{1}\,\bar{1}$)

Yuchen Shi, Alexei A. Zakharov, Ivan Gueorguiev Ivanov, Gholamreza Yazdi, Mikael Syväjärvi, Rositsa Yakimova, and Jianwu Sun*

Graphene layers grown on the C-face SiC exhibit quite different structural and electronic properties compared with those grown on the Si-face SiC. Herein, the growth and structural properties of graphene on the off-axis C-face 3C-SiC($\bar{1}\,\bar{1}\,\bar{1}$) are studied. The as-grown 4° off-axis 3C-SiC($\bar{1}\,\bar{1}\,\bar{1}$) exhibits highly periodic steps with step height of ≈0.75 nm and terrace width of ≈50 nm. After annealing at 1800 °C under 850 mbar argon atmosphere, relatively uniform large graphene domains can be grown. The low-energy electron microscopy (LEEM) results demonstrate that one monolayer (ML) to four-ML graphene domains are grown over several micrometers square, which enables us to measure micro low-energy electron diffraction (μ-LEED) on the single graphene domain. The μ-LEED pattern collected on the monolayer domain mainly exhibits four sets of graphene (1 × 1) spots, indicating the presence of graphene grains with different azimuthal orientations in the same graphene sheet. Raman spectra collected on the graphene domains show rather small D peaks, indicating the presence of less defects and higher crystalline quality of the graphene layers grown on the C-face off-axis 3C-SiC($\bar{1}\,\bar{1}\,\bar{1}$).

1. Introduction

Sublimation growth of graphene on silicon carbide (SiC) is a promising way to produce high-quality, large-scale graphene for electronic and optoelectronic applications without the requirement of extra transfer process, and thus has been extensively investigated during the past decades.[1–5] SiC has two polar faces, which are Si-face and C-face for (0001) and (000$\bar{1}$) in

Dr. Y. Shi, Dr. I. G. Ivanov, Dr. G. Yazdi, Dr. M. Syväjärvi,
Prof. R. Yakimova, Dr. J. Sun
Department of Physics, Chemistry and Biology (IFM)
Linköping University
Linköping SE-58183, Sweden
E-mail: jianwu.sun@liu.se

Dr. A. A. Zakharov
MAX IV Laboratory
Fotongatan 2, Lund SE-22 484, Sweden

hexagonal SiC, (111), and ($\bar{1}\,\bar{1}\,\bar{1}$) in cubic SiC (3C-SiC), respectively. Graphene layers grown on the C-face hexagonal SiC (4H- or 6H-SiC) display only a linearly dispersed π-band in the vicinity of Dirac point closed to the Fermi level, thus behaving like an isolated graphene.[6–8] It has been shown that such graphene layers exhibit higher mobility parameters than that on the Si-face, making graphene/C-face SiC a promising material for the practical applications.[9–11] The reason for this behavior is ascribed to that graphene layers are electronically decoupled between adjacent rotated graphene sheets, which has been interpreted by a high density of rotational faults.[6,7] Contrary to this result, other works reported that rotational domains laterally form within the same graphene layer instead of between the adjacent layers, and the adjacent layers are still in AB-stacking.[12,13]

Alternatively, 3C-SiC is a suitable substrate for the epitaxial growth of large-area multilayer graphene, which is also an attractive material for semiconductor devices such as metal–oxide–semiconductor field-effect transistors (MOSFETs).[14–16] Due to the lack of C-face 3C-SiC substrates, there are very few works devoted to investigating the growth of graphene on the C-face on-axis 3C-SiC. Although some reported results showed similar morphology to the graphene grown on the C-face hexagonal SiC,[17,18] the structural properties of graphene layers have not been well discussed. A recent work reported that few-layer graphene grown on the C-face on-axis 3C-SiC contain azimuthal rotation that occurs between adjacent domains within the same sheet rather than vertically in the stack.[19]

It is known that graphene grown on C-face hexagonal SiC always contains smaller domains with a larger distribution in the number of graphene layers than on the Si-face.[12,20–24] So far, it is still challenging to control the graphene thickness and uniformity on the C-face SiC. Also, graphene grown on the C-face on-axis 3C-SiC has the same issue as that on the C-face hexagonal SiC.[18,19] Moreover, the as-grown on-axis 3C-SiC layers are usually characterized by structural defects such as double-positioning boundaries (DPBs),[25–28] which would negatively affect the growth of graphene. Most recently, we have demonstrated that single-domain C-face 3C-SiC single crystal can be grown on off-axis 4H-SiC substrates and its crystalline quality has been significantly improved.[29] This allows

ADVANCED
SCIENCE NEWS
www.advancedsciencenews.com

physica
pss b
status
solidi
www.pss-b.com

us to grow graphene domains (over several square micrometers) on the C-face 3C-SiC. Moreover, we have demonstrated that the off-oriented Si-face 3C-SiC enabled a fully elimination of step bunching and allowed the growth of uniform large-area graphene.[30] However, it is still unknown whether this growth method can be applied in the case of off-oriented C-face 3C-SiC or not.

In this work, we grow graphene layers on the off-axis C-face 3C-SiC(111) using sublimation technique.[31] The surface morphology before and after the growth of graphene was characterized by atomic force microscopy (AFM). The number of graphene layers was determined by low-energy electron microscopy (LEEM). The surface structural properties of graphene were studied by micro low-energy electron diffraction (μ-LEED). The crystalline quality of graphene layers was demonstrated by Raman spectroscopy.

2. Experimental Section

Off-axis C-face 3C-SiC(111) samples were grown on the C-face 4° off-axis 4H-SiC(0001) substrates. **Figure 1** schematically shows the structural differences between the off-axis and on-axis faces of the 3C-SiC substrate. For the growth of graphene, a 300–400 μm-thick free-standing 3C-SiC crystals were prepared by polishing the 4H-SiC substrate. To remove contaminations and oxide from the surface, the 3C-SiC crystal was gradually cleaned by acetone, ethanol, $H_2O:NH_3:H_2O_2$ (5:1:1), $H_2O:HCl:H_2O_2$ (6:1:1), and hydrofluoric acid (HF).[31] For the growth of graphene, the sample was annealed at 1800 °C with a ramping rate of 25 °C min⁻¹ under 850 mbar argon atmosphere in an inductively heated furnace.[3,30] After annealing at the target temperature for 5 min, the sample was cooled down to the room temperature naturally by switching off the system.
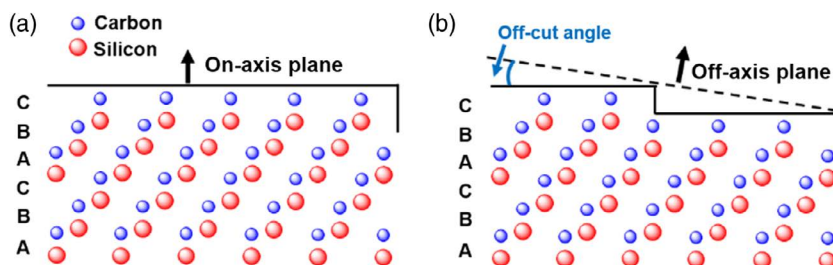
Figure 1. A schematic illustration showing the structural differences between the a) on-axis and b) off-axis faces of the substrate.
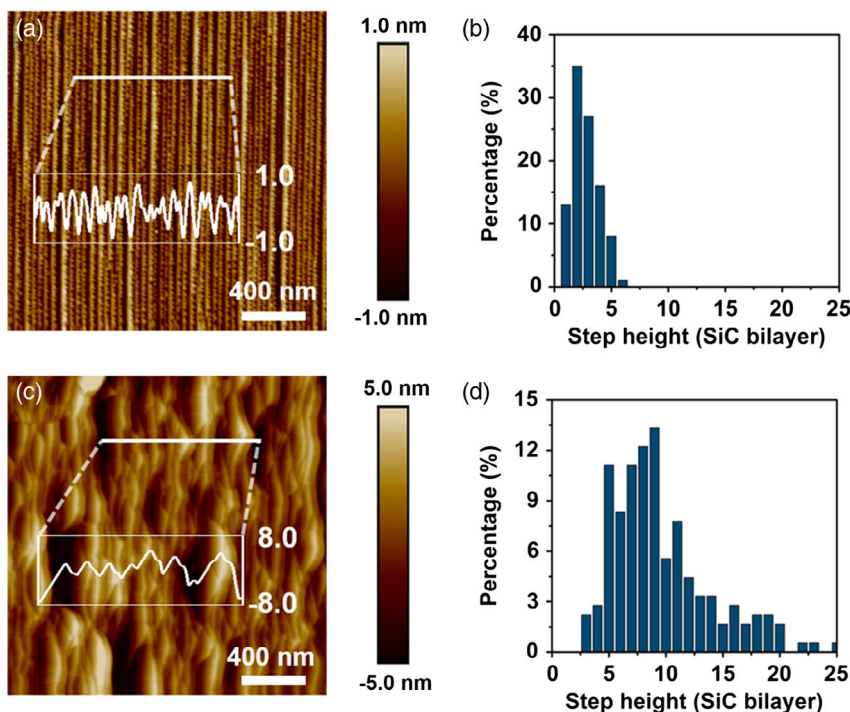
Figure 2. AFM topography $2 \times 2 \, \mu m^2$ images and histograms of the statistic step heights for a,b) the pristine off-axis C-face 3C-SiC and c,d) the graphene sample grown on the off-axis C-face 3C-SiC at 1800 °C for 5 min. The step height profiles of the indicated lines with a dimension of 1 μm are shown in the insets of parts (a) and (c).

The surface morphology was characterized before and after the growth of graphene by AFM in tapping mode. LEEM and LEED images were conducted using the SPELEEM instrument at beamline I311 in the MAX-IV synchrotron radiation laboratory, Lund, Sweden. To remove surface contamination before measurements, the samples were annealed in situ at 600 °C for 20 min. The µ-LEED patterns were collected with a probing area of 500–1000 nm. Raman spectra were measured using a micro-Raman setup with 532 nm laser line excitation. The laser beam passed through a 100× microscope objective, resulting in a spot of diameter ≈800 nm focusing on the sample. The spectral resolution was around ≈5.5 cm^{-1} using a monochromator with 600 grooves mm^{-1} grating coupled to a charge-coupled device (CCD) camera.

3. Results and Discussion

Figure 2 compares the surface morphologies of the pristine off-axis C-face 3C-SiC and graphene grown on C-face 3C-SiC. The as-grown C-face 3C-SiC is characterized by highly periodic steps with step height of ≈0.75 nm and terrace width of ≈50 nm, as shown in Figure 2a and the inset. The statistical histogram of step heights (Figure 2b) on the C-face 3C-SiC confirms that most of the steps are distributed around 0.75 nm height, which

corresponds to three Si-C bilayers or one-3C-SiC unit cell. In addition, the terraces/steps are straight and have length in tens or even hundreds of micrometers, indicating that the 3C-SiC was grown on off-axis 4H-SiC substrate by a step-flow growth mode without step-bunching or DPB formation.[29]

Figure 2c shows the surface morphology of the graphene sample grown on off-axis C-face 3C-SiC. It contains largely distributed terrace widths of 100–200 nm and step heights of 1–5 nm. The statistical histogram (Figure 2d) of step heights confirms that the steps are distributed around 3–25 Si-C bilayers, which correspond to the height of 0.75–6.25 nm. Those large steps were formed due to the step-bunching process, which is related to minimizing surface free energy during the sublimation process of the graphene growth.[2]

LEEM and µ-LEED measurements were used to further characterize the thickness and structural properties of graphene grown on off-axis C-face 3C-SiC. **Figure 3**a shows a typical LEEM image measured on the graphene/C-face 3C-SiC sample with a field of view of 30 µm. Few-layer graphene regions with different thicknesses ranging from one monolayer (1ML) to four-monolayer (4ML) are observed and they are relatively uniform over several square micrometers, compared with graphene grown on the C-face on-axis hexagonal SiC reported previously.[19,32] The thicknesses of graphene domains were
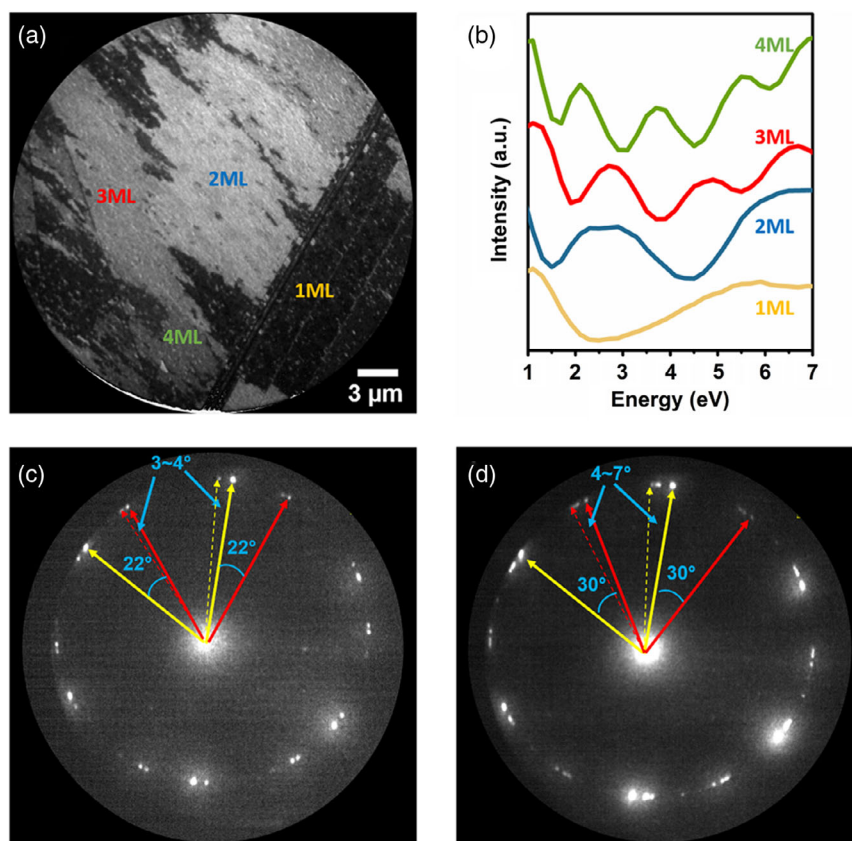
Figure 3. a) LEEM image of the graphene grown on the off-axis C-face 3C-SiC recorded in the field of view of 30 µm with an electron energy of 3.0 eV, showing from 1ML to 4ML graphene domains. b) The electron reflectivity curve collected from the color-labeled regions in part (a). µ-LEED patterns collected on the c) monolayer and d) bilayer domains in the LEEM image, respectively, with a kinetic energy of 52.0 eV. A probing area of 500–1000 nm was used during µ-LEED measurements.

determined by the reflectivity curves shown in Figure 3b, which were collected from the labeled regions in Figure 3a. The number of graphene layers is determined by the number of dips in electron reflectivity.[33] As shown in Figure 3c, the μ-LEED pattern collected on the monolayer domain mainly exhibits four sets of graphene (1 × 1) spots, indicating the presence of the graphene grains with different azimuthal orientations in this monolayer graphene. With respect to the one set of brightest graphene (1 × 1) spots (denoted by solid yellow arrows in Figure 3c), there is one set of weaker (1 × 1) spots that are rotated clockwise around 22° (denoted by solid red arrows in Figure 3c). This angle is consistent with angles reported before, suggesting the presence of rotational disorders in this monolayer graphene.[19,20] Moreover, two other sets of darker (1 × 1) spots indicated by red and yellow dash arrows are rotated around 3°–4° with respect to these two sets of (1 × 1) spots indicated by the red and yellow solid arrows (Figure 3c). This small angle is reminiscent of the rotation of ±2.2° reported on the graphene grown on C-face 4H-SiC.[6] It is worth to note that the large-area coverage of ML graphene (over several square micrometers) enables us to measure μ-LEED pattern on the monolayer region. The μ-LEED pattern of the ML graphene indicates azimuthal rotation occurs between adjacent grains within this monolayer graphene.

Figure 3d shows the μ-LEED pattern collected on the bilayer domain. A set of (1 × 1) spots are rotated at an angle of 30° with respect to the brightest (1 × 1) spots, as indicated by red arrows. The previous reported results showed that a twist angle of around 35° and 20° was observed in the bilayer graphene.[20,34] As shown in Figure 3d, a series of (1 × 1) spots with small rotational angles ranging from around 4°–7° were also observed. Luxmi et al. also reported that such small rotational angles around ≈6°–13° (most typically at ≈7°) were observed on graphene grown on C-face hexagonal SiC.[32]
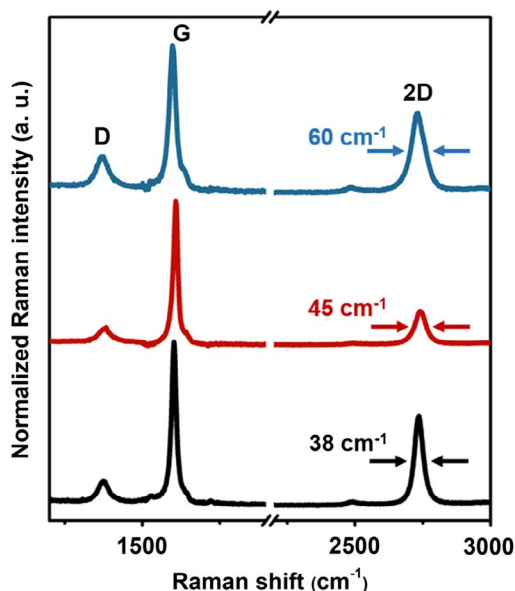
Raman measurements were performed to further investigate the crystalline quality of graphene layers. **Figure 4** shows three representative Raman spectra collected on different areas on the sample surface, which show typical G and 2D peaks of graphene. It has been proposed that the full width at half maximum (FWHM) of 2D peak increases with increase in the number of graphene layers.[35] Three spectra with 2D FWHM of 38, 45, and $60\,cm^{-1}$ implies that the Raman spectra are collected on graphene domains with different thicknesses, as observed in the LEEM image (Figure 3a). The defect-activated D peak is present in all of the spectra and the intensity ratio of D to G peak is related to the defect density. In our spectra, weak D peaks are observed, indicating the presence of less defects and higher crystalline quality of C-face graphene layers compared with the published results.[17,21]

4. Conclusions

In summary, we have studied the growth and structural properties of graphene on the off-axis C-face 3C-SiC($\bar{1}\,\bar{1}\,\bar{1}$). Large graphene domains with the thicknesses ranging from 1ML to 4ML were obtained. Particularly, graphene domains are relatively homogeneous over several square micrometers compared with few-layer graphene grown on on-axis hexagonal SiC. μ-LEED measurements revealed that the monolayer graphene domain contains several azimuthal rotations, which are considered as the laterally rotational grains in the same graphene sheet. The bilayer graphene contains two sets of graphene (1 × 1) spots that are rotated 30° with respect to each other and a series of small azimuthal rotational spots ranging from around 4° to 7° are also observed.

Conflict of Interest

The authors declare no conflict of interest.

Figure 4. Raman spectra measured on different areas of the graphene sample. A reference spectrum of the 3C-SiC substrate is subtracted from the spectra to eliminate the contribution from the second-order Raman bands of 3C-SiC overlapping the D and G peaks.

Keywords

azimuthal orientations, C-face 3C-SiC, epitaxial graphene, off-axis substrates

[1] C. Virojanadara, M. Syväjarvi, R. Yakimova, L. I. Johansson, A. A. Zakharov, T. Balasubramanian, *Phys. Rev. B* **2008**, *78*, 245403.

[2] G. R. Yazdi, R. Vasiliauskas, T. Iakimov, A. Zakharov, M. Syväjärvi, R. Yakimova, *Carbon* **2013**, *57*, 477.

[3] K. V. Emtsev, A. Bostwick, K. Horn, J. Jobst, G. L. Kellogg, L. Ley, J. L. McChesney, T. Ohta, S. A. Reshanov, J. Rohrl, E. Rotenberg, A. K. Schmid, D. Waldmann, H. B. Weber, T. Seyller, *Nat. Mater.* **2009**, *8*, 203.

[4] H. C. Wu, A. N. Chaika, T. W. Huang, A. Syrlybekov, M. Abid, V. Y. Aristov, O. V. Molodtsova, S. V. Babenkov, D. Marchenko, J. Sánchez-Barriga, P. S. Mandal, *ACS Nano* **2015**, *9*, 8967.

[5] D. Pierucci, H. Sediri, M. Hajlaoui, E. Velez-Fort, Y. J. Dappe, M. G. Silly, R. Belkhou, A. Shukla, F. Sirotti, N. Gogneau, A. Ouerghi, *Nano Res.* **2015**, *8*, 1026.

[6] J. Hass, F. Varchon, J. E. Millan-Otoya, M. Sprinkle, N. Sharma, W. A. de Heer, C. Berger, P. N. First, L. Magaud, E. H. Conrad, *Phys. Rev. Lett.* **2008**, *100*, 125504.

[7] J. Hass, R. Feng, J. E. Millán-Otoya, X. Li, M. Sprinkle, P. N. First, W. A. de Heer, E. H. Conrad, C. Berger, *Phys. Rev. B* **2007**, *75*, 214109.

[8] D. A. Siegel, C. G. Hwang, A. V. Fedorov, A. Lanzara, *Phys. Rev. B* **2010**, *81*, 241417(R).

[9] J. L. Tedesco, B. L. VanMil, R. L. Myers-Ward, J. M. McCrate, S. A. Kitt, P. M. Campbell, G. G. Jernigan, J. C. Culbertson, C. R. Eddy, D. K. Gaskill, *Appl. Phys. Lett.* **2009**, *95*, 122102.

[10] C. Berger, Z. M. Song, X. B. Li, X. S. Wu, N. Brown, C. Naud, D. Mayou, T. B. Li, J. Hass, A. N. Marchenkov, E. H. Conrad, P. N. First, W. A. de Heer, *Science* **2006**, *312*, 1191.

[11] Y. M. Lin, C. Dimitrakopoulos, D. B. Farmer, S. J. Han, Y. Q. Wu, W. J. Zhu, D. K. Gaskill, J. L. Tedesco, R. L. Myers-Ward, C. R. Eddy, A. Grill, P. Avouris, *Appl. Phys. Lett.* **2010**, *97*, 112107.

[12] L. I. Johansson, S. Watcharinyanon, A. A. Zakharov, T. Iakimov, R. Yakimova, C. Virojanadara, *Phys. Rev. B* **2011**, *84*, 125405.

[13] L. I. Johansson, R. Armiento, J. Avila, C. Xia, S. Lorcy, I. A. Abrikosov, M. C. Asensio, C. Virojanadara, *Sci. Rep.* **2014**, *4*, 4157.

[14] M. Bhatnagar, B. Jayant Baliga, *IEEE Trans. Electron Devices* **1993**, *40*, 645.

[15] C. I. Harris, S. Savage, A. Konstantinov, M. Bakowski, P. Ericsson, *Appl. Surf. Sci.* **2001**, *184*, 393.

[16] A. Schöner, M. Krieger, G. Pensl, M. Abe, H. Nagasawa, *Chem. Vap. Deposit.* **2006**, *12*, 523.

[17] H. Fukidome, S. Abe, R. Takahashi, K. Imaizumi, S. Inomata, H. Handa, E. Saito, Y. Enta, A. Yoshigoe, Y. Teraoka, M. Kotsugi, T. Ohkouchi, T. Kinoshita, S. Ito, M. Suemitsu, *Appl. Phys. Express* **2011**, *4*, 115104.

[18] V. Darakchieva, A. Boosalis, A. A. Zakharov, T. Hofmann, M. Schubert, T. E. Tiwald, T. Iakimov, R. Vasiliauskas, R. Yakimova, *Appl. Phys. Lett.* **2013**, *102*, 213116.

[19] C. Bouhafs, V. Stanishev, A. A. Zakharov, T. Hofmann, P. Kühne, T. Iakimov, R. Yakimova, M. Schubert, V. Darakchieva, *Appl. Phys. Lett.* **2016**, *109*, 203102.

[20] L. Johansson, C. Xia, J. Hassan, T. Iakimov, A. Zakharov, S. Watcharinyanon, R. Yakimova, E. Janzén, C. Virojanadara, *Crystals* **2013**, *3*, 1.

[21] C. E. Giusca, S. J. Spencer, A. G. Shard, R. Yakimova, O. Kazakova, *Carbon* **2014**, *69*, 221.

[22] I. Razado-Colambo, J. Avila, C. Chen, J. P. Nys, X. Wallart, M. C. Asensio, D. Vignaud, *Phys. Rev. B* **2015**, *92*, 035105.

[23] Y. Hu, Y. Zhang, H. Guo, L. Chong, Y. Zhang, *Mater. Lett.* **2016**, *164*, 655.

[24] B. Sharma, T. Schumann, M. H. de Oliveira, J. M. J. Lopes, *Phys. Status Solidi A* **2017**, *214*, 1600721.

[25] L. Latu-Romain, D. Chaussende, M. Pons, *Cryst. Growth Des.* **2006**, *6*, 2788.

[26] M. Soueidan, G. Ferro, O. Kim-Hak, F. Cauwet, B. Nsouli, *Cryst. Growth Des.* **2008**, *8*, 1044.

[27] O. Kim-Hak, G. Ferro, J. Dazord, M. Marinova, J. Lorenzzi, E. Polychroniadis, P. Chaudouët, D. Chaussende, P. Miele, *J. Cryst. Growth* **2009**, *311*, 2385.

[28] R. Vasiliauskas, S. Juillaguet, M. Syväjärvi, R. Yakimova, *J. Cryst. Growth* **2012**, *348*, 91.

[29] Y. C. Shi, V. Jokubavicius, P. Höjer, I. G. Ivanov, G. R. Yazdi, R. Yakimova, M. Syväjärvi, J. Sun, *J. Phys. D: Appl. Phys.* **2019**, *52*, 345103.

[30] Y. C. Shi, A. A. Zakharov, I. G. Ivanov, G. R. Yazdi, V. Jokubavicius, M. Syväjärvi, R. Yakimova, J. Sun, *Carbon* **2018**, *140*, 533.

[31] V. Jokubavicius, G. R. Yazdi, R. Liljedahl, I. G. Ivanov, R. Yakimova, M. Syväjärvi, *Cryst. Growth Des.* **2014**, *14*, 6514.

[32] Luxmi, N. Srivastava, G. He, R. M. Feenstra, P. J. Fisher, *Phys. Rev. B* **2010**, *82*, 235406.

[33] H. Hibino, H. Kageshima, F. Maeda, M. Nagase, Y. Kobayashi, H. Yamaguchi, *Phys. Rev. B* **2008**, *77*, 075413.

[34] T. Ohta, T. E. Beechem, J. T. Robinson, G. L. Kellogg, *Phy. Rev. B* **2012**, *85*, 075415.

[35] A. C. Ferrari, J. C. Meyer, V. Scardaci, C. Casiraghi, M. Lazzeri, F. Mauri, S. Piscanec, D. Jiang, K. S. Novoselov, S. Roth, A. K. Geim, *Phys. Rev. Lett.* **2006**, *97*, 187401.